Available online at www.sciencedirect.com
ScienceDirect
Ocean Modelling 17 (2007) 183–198
Ocean Modelling
www.elsevier.com/locate/ocemod

# Overshootings and spurious oscillations caused by biharmonic mixing

Éric J.M. Delhez [a,*], Éric Deleersnijder [b]

[a] Université de Liège, LTAS – Modélisation et Méthodes Mathématiques, Sart Tilman B37, B-4000 Liège, Belgium
[b] Université catholique de Louvain, G. Lemaitre Institute of Astronomy and Geophysics (ASTR) & Centre for Systems Engineering and Applied Mechanics (CESAME), 4 Avenue G. Lemaître, B-1348 Louvain-la-Neuve, Belgium

Received 24 November 2006; received in revised form 19 January 2007; accepted 19 January 2007
Available online 31 January 2007

**Abstract**

Biharmonic mixing is often used in large scale numerical models of the ocean because of its scale selectivity; it effectively damps small scale noise and leaves the large scale dynamics nearly unaffected. The biharmonic operator lacks however positiveness and monotonicity and can therefore produce unphysical results exhibiting spurious overshootings and oscillations. This problematic behaviour cannot be avoided by the addition of an ordinary Laplacian diffusion term. It appears in both continuous and discrete approaches/solutions in both unbounded and bounded domains.

The overshootings and oscillations are induced by the strong damping of the smaller scale modes and are therefore comparable to the Gibbs' phenomenon. With appropriate boundary conditions, the variance of the field decreases monotonically and the oscillations are expected to remain small. The lack of positiveness is however a severe drawback for (dynamic) tracer studies.


*Keywords:* Biharmonic mixing; Numerical model; Ocean dynamics; Monotonicity; Positiveness

## 1. Introduction

Mixing is an important process of the dynamics of the ocean and the atmosphere. Its appropriate parameterization in numerical models is however a tricky task because diffusion must not only reflect the physical processes associated with sub-grid scale features but it must also damp the numerical noise created by the numerical scheme. As a result, most generic ocean and atmosphere circulation models include options to select among various mixing parameterizations (e.g. Smith and Gent, 2002; Griffies et al., 2004). For instance, users of the OPA ocean model system (Madec et al., 1991, 1999; Foujols et al., 2000) can choose among a Laplacian diffusion, a Gent and McWilliams formulation (Gent and McWilliams, 1990; Gent et al., 1995) or biharmonic

* Corresponding author. Tel.: +32 43669419; fax: +32 43669489.
*E-mail address:* E.Delhez@ulg.ac.be (É.J.M. Delhez).

1463-5003/$ - see front matter © 2007 Elsevier Ltd. All rights reserved.
doi:10.1016/j.ocemod.2007.01.002

mixing (in different coordinate systems for some options) to parameterize the lateral diffusion of momentum and tracers.

The introduction of a biharmonic mixing term is often advocated for its ability to act more efficiently on the smallest scales, leaving larger scales that are well resolved by the grid relatively untouched (Griffies and Hallberg, 2000; Batteen et al., 2000; Hunke et al., 2005). This property explains the success of the biharmonic approach in global atmospheric models (where lateral boundary conditions do not hamper the implementation of the associated fourth order operator) and the increasing use of this kind of parameterization in a wide range of ocean simulations (e.g. Willebrand et al., 2001; Xing and Davies, 2002; Lee and Coward, 2003; Myers and Deacu, 2004; Simmons et al., 2004; Oka and Hasumi, 2006; Shaw and Chao, 2006).

Biharmonic mixing also appears in the analysis of high order advection schemes. The QUICK advection scheme (Leonard, 1979; Holland et al., 1998; Webb et al., 1998) and the third-order upwind scheme (e.g. Holland et al., 1998), for instance, both amounts to introducing a biharmonic mixing term that damps out short wavelength components and helps to limit the number of spurious maxima and minima in the solution.

While the more traditional Laplacian formulation of diffusion relies on a well-established understanding of diffusion fluxes flowing against the concentration gradients, similar physical interpretations are missing for the biharmonic formulation and problems associated with biharmonic mixing are reported occasionally. In Foujols et al. (2000), one can read that 'the user [of OPA] should be aware that the biharmonic operator does not insure the conservation of positivity, contrary to the Laplacian one'. Titz et al. (2004) mention that a correction term is needed to address this problem. Merryfield and Holloway (2003) report the production of overshootings by the biharmonic operator in their simulation of ice thickness. DiBattista et al. (2001) provide a detailed discussion of the steepening of flow features in a quasi-geostrophic model. Griffies (2004) mentions that, with a non-linear equation of state, the possible occurrence of upgradient fluxes of temperature and salinity from a biharmonic operator leads to sign-indefinite cabbeling, which is unphysical.

The purpose of this note is to document the peculiar behaviour of biharmonic mixing, better understand when and why problems appear and warn potential users of the possible occurrence of some unphysical results.

## 2. Laplacian and biharmonic formulations

In numerical models, the general form of the diffusion flux $\mathbf{J}$ of a scalar property $C$ is usually given by

$$\mathbf{J} = -\mathbf{K}\cdot\nabla C + \nabla_{\mathrm{h}}(\kappa_4\nabla_{\mathrm{h}}^2 C) \tag{1}$$

where $\mathbf{K}$ is the Laplacian diffusion tensor, $\kappa_4$ is the horizontal coefficient for biharmonic mixing and $\nabla_{\mathrm{h}}$ is the horizontal or isopycnic part of the $\nabla$ ('nabla' or 'del') differential operator. The symmetric tensor $\mathbf{K}$ is generally non-isotropic to reflect the vertical stratification and its principal axes are usually set in relation with sloping, neutral surfaces (e.g. Gent and McWilliams, 1990). The resulting diffusion term in the evolution equation for $C$ is basically three-dimensional. On the contrary, since the main purpose of biharmonic mixing is to damp numerical oscillations, the corresponding term is generally two-dimensional only and the coefficient $\kappa_4$ is assumed to be constant or to vary spatially with the local grid size (e.g. Griffies and Hallberg, 2000).

The effect of the two terms of (1) on the dynamics of a tracer can be demonstrated by the analysis of the Fourier modes of the constant coefficient version of the one-dimensional conservation equation for the scalar $C$ when diffusion is the only relevant process, i.e.

$$\frac{\partial C}{\partial t} = \kappa_2\frac{\partial^2 C}{\partial x^2} - \kappa_4\frac{\partial^4 C}{\partial x^4} \tag{2}$$

where $\kappa_2$ is the constant Laplacian diffusivity. This equation has wavelike solutions in the form

$$C(t,x) \propto \exp[\sigma t + \mathrm{i}kx] \tag{3}$$

with wavenumber $k$ and wavelength $2\pi/k$ for

$$\sigma = -\kappa_2 k^2 - \kappa_4 k^4 \tag{4}$$

The dispersion relation (4) clearly shows that both Laplacian diffusion and biharmonic mixing terms induce an exponential damping of all Fourier modes. As was claimed above, Laplacian diffusion dominates for small wave numbers, i.e. large wavelengths, while biharmonic mixing more actively damps small scale features.

The scale selectivity of biharmonic mixing is preserved in the discrete case; when centered differences are used in space to discretize (2) on a uniform grid of spacing $\Delta$, the spindown times $\tau_L$ and $\tau_b$ for Laplacian diffusion and biharmonic mixing are given by (see Semtner and Mintz (1977) or Eq. (20)), respectively,

$$\tau_L = \frac{1}{\kappa_2}\left[\frac{2}{\Delta}\sin(k\Delta/2)\right]^{-2} \tag{5}$$

and

$$\tau_b = \frac{1}{\kappa_4}\left[\frac{2}{\Delta}\sin(k\Delta/2)\right]^{-4} \tag{6}$$

Consequently, the longer waves, which are also better resolved, have longer spindown times with the biharmonic mixing formulation.

## 3. Overshootings and wiggles

The properties of biharmonic mixing shortly discussed above render this parameterization very attractive for numerical models. However, since biharmonic fluxes are not guaranteed to be downgradient, unphysical behaviours can be expected.

As a demonstration of these problems, we consider the biharmonic mixing of a patch of a passive tracer in the infinite one-dimensional domain $x \in (-\infty, +\infty)$ under the effect of biharmonic mixing. Mathematically, one has

$$\begin{cases} \dfrac{\partial C}{\partial t} = -\kappa_4 \dfrac{\partial^4 C}{\partial x^4} \\ C(0,x) = C_0(x) \end{cases} \tag{7}$$

where $C_0(x)$ is the initial distribution of the concentration and the diffusion coefficient $\kappa_4 > 0$ is assumed to be a constant.

Snapshots of the concentration distribution obtained by the integration forward in time of (7) from the initial concentration field

$$C_0(x) = \begin{cases} 0 & \text{for } |x| > 1 \\ 1 & \text{for } |x| < 1 \end{cases} \tag{8}$$

are shown in Fig. 1 (for $\kappa_4 = 1$). The concentration shows spatial oscillations with overshootings and undershootings that are in clear contradiction with the usual understanding of the dynamics of diffusion. The oscillations develop at very early times in the vicinity of the points of discontinuity of the initial distribution. The undershootings rapidly reach about 5% of the initial concentration jump. Their amplitude remains then nearly constant in time while the associated oscillations progressively moves along the $x$ axis. At $x = 0$, the disturbances produced by the two edges of the initial distribution combine to create an overshooting of about 10%. Of course, such a pathological behaviour does not appear with the harmonic diffusion (not shown).

It must be stressed that the oscillations, over- and under-shoots appearing in Fig. 1 are not a numerical artefact or induced by a deficient resolution procedure (which is explained in Appendix A). Also, while the over- and under-shoots are obviously triggered by the discontinuities in the initial concentration field, the same behaviour can be observed with arbitrary initial conditions, including Gaussian like distributions.

To understand the origin of the pathological behaviour of biharmonic mixing, it is instructive to solve the initial value problem (7) by taking the Fourier transform of the problem with respect to the spatial variable $x$. The problem becomes then

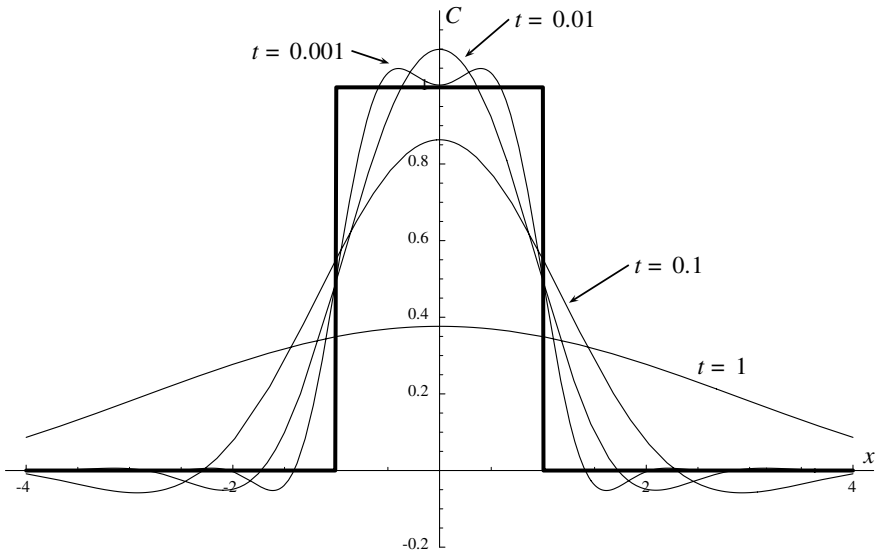


Fig. 1. Snapshots of the concentration field $C$ for a pure biharmonic diffusion ($\kappa_4 = 1$) at time $t = 0$ (thick curve), $t = 0.001$, $t = 0.01$, 0.1 and 1 (arbitrary units).

$$\begin{cases} \dfrac{\partial \widetilde{C}}{\partial t} = -\kappa_4 k^4 \widetilde{C} \\ \widetilde{C}(0,k) = \widetilde{C}_0(k) \end{cases} \tag{9}$$

where $k$ is the wave number and where

$$\widetilde{C}(t,k) = \mathscr{F}_x[C(t,x)] \tag{10}$$

and

$$\widetilde{C}_0(k) = \mathscr{F}_x[C_0(x)] \tag{11}$$

denote the Fourier transform of the concentration field at time $t$ and at the initial time. From (9), the solution of the problem is easily obtained as

$$C(t,x) = \mathscr{F}_x^{-1}[\widetilde{C}(t,k)] = \mathscr{F}_x^{-1}[\widetilde{C}_0(k)\mathrm{e}^{-\kappa_4 k^4 t}] \tag{12}$$

where $\mathscr{F}_x^{-1}$ is the inverse Fourier transform operator.

The general form of the solution (12) shows that, as expected, diffusion leads to the exponential decay with time of all spatial Fourier modes of the initial distribution. Therefore, the variance of the concentration field decreases monotonically. Thanks to the $k^4$ dependency of the exponential appearing in (12), the modes with a high wave number are strongly damped while the smaller wave number modes are nearly unaffected. Biharmonic diffusion behaves thus like a very efficient low-pass filter whose transfer function is given by

$$\widetilde{H}(k) = \mathrm{e}^{-\kappa_4 k^4 t} \tag{13}$$

Fig. 2 shows the effect of this filtering on the spectrum of the rectangle function (8) used in Fig. 1. For comparison purposes, the corresponding filtering induced by the Laplacian diffusion operator is also plotted. The damping of high frequency modes is much less severe with the Laplacian diffusion. The corresponding transfer function decreases also much less rapidly than that of the biharmonic mixing which appears to introduce a clear cut-off frequency with a rapid decrease of the transfer function around

$$k_{\mathrm{cf}} = (\kappa t)^{-1/4} \tag{14}$$

This demonstrates, once again, the scale selectivity of the biharmonic mixing.

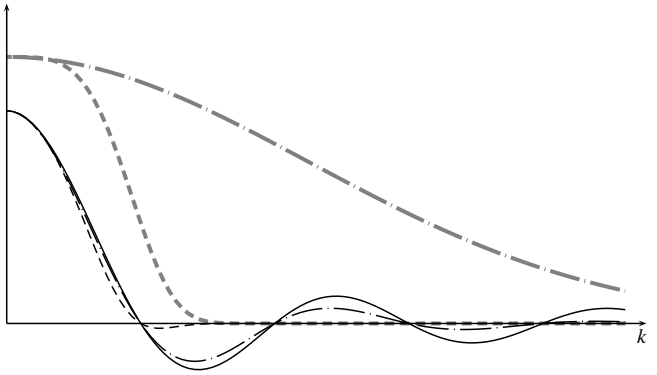


Fig. 2. Fourier transform of the rectangle function (8) (thin solid), filtering by the biharmonic diffusion for $\kappa_4 = 1$ and $t = 0.01$ (thin dashed), corresponding filtering by Laplacian diffusion for $\kappa_2 = 1$ (thin dot-dashed), corresponding transfer functions for the biharmonic (thick dashed) and Laplacian diffusion (thick dot-dashed).

From (12), one can also notice that the behaviour of the solution is insensitive to the value of the diffusion coefficient; if the diffusion coefficient is doubled, the same concentration field will just evolve two times faster.

The cut-off frequency introduced by the transfer function (13) is responsible for the pathological behaviour of biharmonic mixing in a way that is very similar to Gibbs' phenomenon for the Fourier series representation of a discontinuous function. In this case, the suppression of higher frequency modes occurs because of the truncation of the full Fourier series as partial sums are considered (e.g. Morse and Feshbach, 1953). In the case of biharmonic mixing, the damping of these modes is a consequence of the dynamics underlying (13). The consequences are however identical: oscillations and lack of positiveness. Interestingly, the oscillations apparent in Fig. 1 exhibit the same behaviour as those associated with Gibbs' phenomenon: their amplitude remains nearly constant while they spread away from regions of sharp gradients. In a way, this is good news as the oscillations remain of small amplitude and do not dominate the solution. Nevertheless, the lack of positiveness can be unacceptable in many applications.

Since Laplacian diffusion does not suffer from the same pathological behaviour as the biharmonic version, it is natural to examine whether the introduction of some level of harmonic diffusion can help to address the problem. To this end, compute the Green function $\mathscr{G}_1$ associated with the mixed harmonic/biharmonic mixing problem, i.e. the solution of

$$\begin{cases} \dfrac{\partial \mathscr{G}_1}{\partial t} = \kappa_2 \dfrac{\partial^2 \mathscr{G}_1}{\partial x^2} - \kappa_4 \dfrac{\partial^4 \mathscr{G}_1}{\partial x^4} \\ \mathscr{G}_1(0,x) = \delta(x) \end{cases} \tag{15}$$

where $\delta$ is the Dirac impulse generalized function. Using the Fourier transform approach introduced above, the Green function can be easily expressed as

$$\mathscr{G}_1(t,x) = \mathscr{F}_x^{-1}[\mathrm{e}^{-(\kappa_2 k^2 + \kappa_4 k^4)t}] \tag{16}$$

The Green function summarizes the dynamics of the (linear) system and can be used to write the solution of the mixed diffusion problem for arbitrary initial conditions $C_0(x)$. One has indeed (e.g. Morse and Feshbach, 1953)

$$C(t,x) = \int_{-\infty}^{+\infty} C_0(u)\mathscr{G}_1(t,x-u)\,\mathrm{d}u \tag{17}$$

With the introduction of the dimensionless variables

$$t_\star = \frac{\kappa_2^2}{\kappa_4} t, \quad x_\star = \sqrt{\frac{\kappa_2}{\kappa_4}} x, \tag{18}$$

the expression (16) becomes

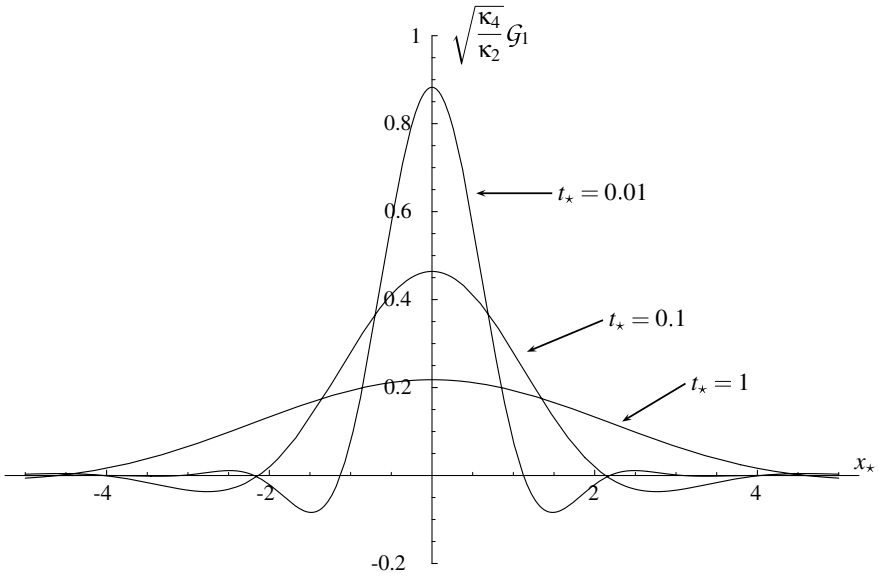


Fig. 3. Snapshots at times $t_\star = 0.01$, 0.1 and 1 of the 1D Green function $\mathcal{G}_1$ for a mixed harmonic/biharmonic diffusion (dimensionless variables).

$$\mathcal{G}_1(t_\star, x_\star) = \frac{1}{\pi}\sqrt{\frac{\kappa_2}{\kappa_4}}\int_0^{+\infty} \cos(k_\star x_\star)\mathrm{e}^{-(k_\star^2+k_\star^4)t_\star}\,\mathrm{d}k_\star \tag{19}$$

Snapshots of the Green function are plotted in Fig. 3. These resulting concentration field shows exactly the same pathological behaviour as in the case of pure biharmonic mixing: the solution exhibits oscillations and lacks positiveness. Since changing the values of $\kappa_2$ and $\kappa_4$ only modifies the characteristic time scale and length scale of the solution but does not affect its qualitative behaviour, it is impossible to get rid of the oscillations by adjusting the diffusion coefficients unless $\kappa_4 = 0$. In particular, it must be clear that, while the introduction of a harmonic diffusion term (consider the scaling of the Green function) reduces the absolute magnitude of the solution, the additional smoothing does not affect the relative size of the oscillations. The bottom line is therefore that the concentration field obtained from arbitrary initial conditions will always exhibit the pathological behaviour discussed above. In particular, the addition of a Laplacian diffusion term is not a valid solution to the problems of overshootings and spurious oscillations appearing in simulations using biharmonic mixing. These problems are intrinsic to the biharmonic operator.

## 4. Generalization to higher dimensions and discrete form

In most numerical models, biharmonic mixing is introduced in the horizontal plane, i.e. in two dimensions. The analysis carried out in the previous section must therefore be extended to higher dimension versions of (15).

Integral representation of the corresponding Green functions are derived in Appendix B in both 2D and 3D cases. Considering the natural symmetry of the problem, only the radial coordinate is involved in the spatial dependency of these Green functions. While less critical than in Fig. 3, negative overshootings are still apparent in Fig. 4 for both 2D and 3D versions of the problem.

Since the introduction of biharmonic mixing term in ocean models is primarily motivated by the need to damp out numerical noise/instabilities, it is also interesting to investigate the effect of this parameterization on the discrete versions of the problems examined above. To this end, we consider a 1D regular mesh with a constant grid size $\Delta$ and use centered differences to approximate the spatial derivatives. We use a mixed approach in which the time is not discretized. The concentration field is then characterized by the concentra-

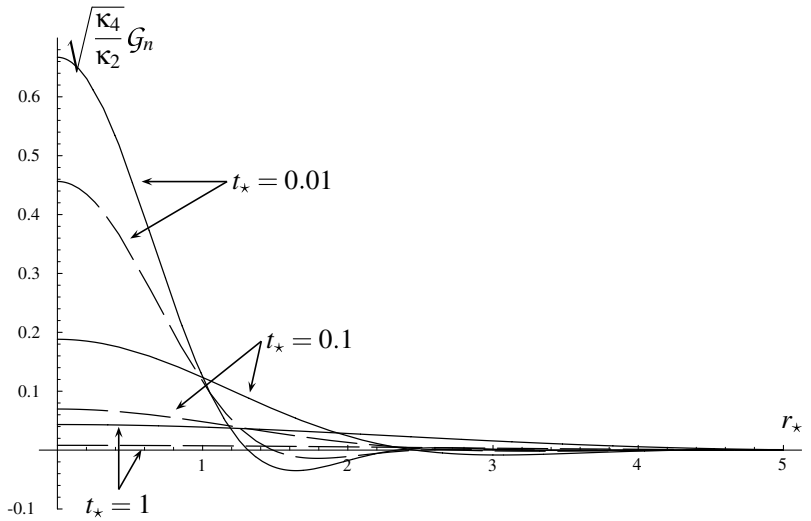


Fig. 4. Snapshots at times $t_\star = 0.01$, 0.1 and 1 of the 2D (solid line) and 3D (dashed line) Green functions $\mathcal{G}_n$ for a mixed harmonic/biharmonic diffusion.

tion $C_j(t)$ at the grid points $x_j = j\Delta$ for $j = 0, \pm 1, \pm 2, \ldots$ The discrete Green function $\mathcal{G}_j^\Delta(t)$ for this system, with both terms of diffusion, can be expressed (see Appendix C) as

$$\mathcal{G}_j^\Delta(t) = \frac{1}{\pi\Delta}\int_0^{+\pi} \exp\left(-\left[\frac{4\kappa_2 \sin^2(k/2)}{\Delta^2} + \frac{16\kappa_4 \sin^4(k/2)}{\Delta^4}\right]t\right)\cos(kj)\,\mathrm{d}k \tag{20}$$

As shown in Fig. 5, this approach does not permit to get rid of the unphysical behaviour of the biharmonic operator: the discrete solution exhibits exactly the same behaviour as the corresponding continuous one.

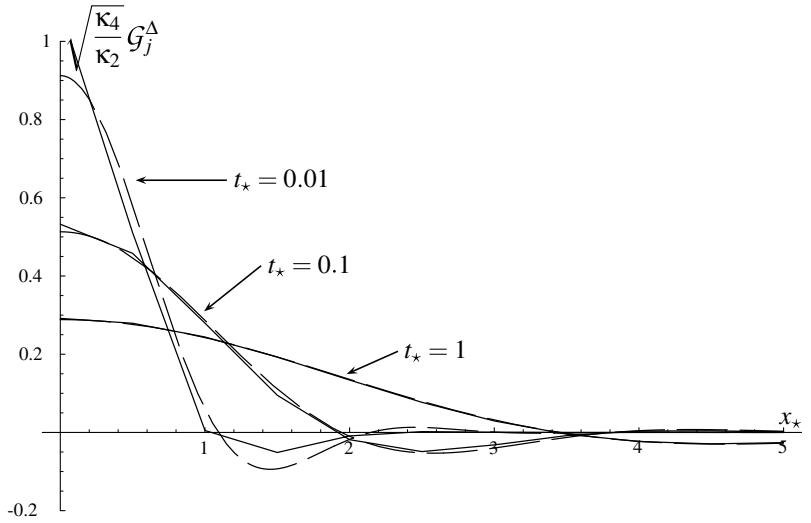


Fig. 5. Snapshots at times at time $t = 0.01$, 0.1 and 1 of the 1D discrete Green function $\mathcal{G}_j^\Delta$ for a pure biharmonic diffusion ($\kappa_4 = 1$) and a grid size $\Delta = 0.5$ (solid line). For comparison, the corresponding continuous solution is also reproduced (dashed line).

## 5. Boundary conditions

The previous computations were carried out in an infinite domain. The same problems of overshootings and spurious oscillations are likely to appear in more realistic simulations in a bounded domain. The results shown by Merryfield and Holloway (2003) in the Appendix of their manuscript form a clear demonstration thereof.

From a mathematical point of view, this comes as no surprise. The Green function $\mathscr{G}_{\text{bounded}}$ of the (continuous or discrete) problem in a bounded domain can indeed be written as

$$\mathscr{G}_{\text{bounded}} = \mathscr{G}_{\text{unbounded}} + \mathscr{G}_{\text{BC}} \tag{21}$$

where $\mathscr{G}_{\text{unbounded}}$ is the Green function in an unbounded domain – as studied above – and $\mathscr{G}_{\text{BC}}$ is a correction of $\mathscr{G}_{\text{unbounded}}$ that takes into account the boundary conditions. Because $\mathscr{G}_{\text{unbounded}}$ is singular at the initial release point and $\mathscr{G}_{\text{BC}}$ is regular in the whole domain (Morse and Feshbach, 1953), the behaviour of the solution in the vicinity of the release point is controlled by $\mathscr{G}_{\text{unbounded}}$ and will therefore exhibit oscillations and negative values as in the unbounded case. The boundary conditions play therefore only a limited part in this issue and cannot be adjusted to damp out the unphysical behaviour of the solution.

What is worse, boundary conditions must also be properly designed to avoid further problems. To design appropriate treatments at solid boundaries, consider the advection–diffusion of a conservative tracer in a bounded domain $V$ with a fixed impermeable boundary $\Gamma$. The corresponding initial value problem with mixed diffusion formulation can be expressed as

$$\begin{cases} \dfrac{\partial C}{\partial t} = -\nabla \cdot \{\mathbf{u}C - \mathbf{K} \cdot \nabla C + \nabla(\kappa_4 \nabla^2 C)\} \\ C(0, \mathbf{x}) = C_0(\mathbf{x}) \end{cases} \tag{22}$$

(assuming for simplicity that the Laplacian diffusion and biharmonic mixing operators both act in all directions) where $C$ is the concentration of the scalar, $\mathbf{u}$ is the divergence-free velocity field and $C_0$ describes the initial distribution field. Requiring that the flux of the material across the impermeable boundary $\Gamma$ vanishes leads to

$$[\mathbf{n} \cdot \{-\mathbf{K} \cdot \nabla C + \nabla(\kappa_4 \nabla^2 C)\}]_{\mathbf{x} \in \Gamma} = 0 \tag{23}$$

where $\mathbf{n}$ is the outward unit normal vector. Obviously, the total mass of the tracer is then conserved and its basin average value $\overline{C}$ is a constant.

When only Laplacian diffusion is considered ($\kappa_4 = 0$), the boundary condition (23) simplifies to

$$[\mathbf{n} \cdot \mathbf{K} \cdot \nabla C]_{\mathbf{x} \in \Gamma} = 0 \tag{24}$$

and is sufficient to solve (22). Provided that $\mathbf{K}$ is positive definite, this condition also ensures that the concentration of the tracer remains positive at any time and location (see Appendix E) and that its spatial variance decreases in time until the gradient of the concentration vanishes everywhere in the domain.

When biharmonic mixing is taken into account, the order of the differential problem (22) increases and an additional boundary condition must be prescribed on $\Gamma$. This can be obtained by considering the deviation $\widehat{C} = C - \overline{C}$ of the concentration with respect to its (constant) basin average value. Taking into account the boundary condition (23), the impermeability of $\Gamma$ and the cancellation of the divergence of the velocity field, one can show (see Appendix) that the spatial variance of the concentration field evolves according to

$$\frac{1}{2}\frac{\mathrm{d}}{\mathrm{d}t}\int_V \widehat{C}^2 \,\mathrm{d}V = \int_\Gamma (\mathbf{n} \cdot \nabla \widehat{C})(\kappa_4 \nabla^2 \widehat{C}) \,\mathrm{d}\Gamma - \int_V \{\nabla \widehat{C} \cdot \mathbf{K} \cdot \nabla \widehat{C} + \kappa_4 (\nabla^2 \widehat{C})^2\} \,\mathrm{d}V \tag{25}$$

As claimed above, the use of a positive definite Laplacian diffusion tensor is sufficient to make the variance of the concentration decreases with time if $\kappa_4 = 0$. In the general case, since the sign of the surface integral in the right-hand side of (25) is indefinite, this requirement on $\mathbf{K}$ must be complemented by the condition $\kappa_4 \geqslant 0$ and the prescription of either of the following boundary conditions:

$$[\kappa_4 \nabla^2 C]_{\mathbf{x} \in \Gamma} = 0 \tag{26}$$

or

$$[\mathbf{n}\cdot(\kappa_4\nabla C)]_{\mathbf{x}\in\Gamma}=0 \tag{27}$$

Obviously, the boundary condition (26) is compatible with the evolution of the solution towards a steady state inhomogeneous solution where the Laplacian of the concentration field is zero while diffusion is expected to make the concentration field tend to a constant value over the domain of interest. With the boundary condition (26), one should therefore rely on the effect of the Laplacian diffusion to induce this expected behaviour of the solution. For this reason, condition (27) should be preferred as it will lead to the progressive smoothing of the concentration field until complete homogenization over the whole domain irrespective of the Laplacian diffusion. This provides the additional boundary condition necessary to solve (22).

Still, while the boundary conditions (23) and (27) appear as sufficient conditions to ensure that the variance decreases with time, they do not prevent spurious oscillations and overshootings from developing. This is clearly demonstrated by Fig. 6 showing snapshots of the solution in $[-1,1]$ of the biharmonic mixing problem

$$\begin{cases}\dfrac{\partial C}{\partial t}=-\dfrac{\partial^4 C}{\partial x^4}\\ C(0,x)=h(x)\\ \left[\dfrac{\partial C}{\partial x}\right]_{x=\pm1}=\left[\dfrac{\partial^3 C}{\partial x^3}\right]_{x=\pm1}=0\end{cases} \tag{28}$$

(where $h(x)$ is the Heaviside 'step' function) which is adapted from Merryfield and Holloway (2003).

The solution of (28) can be expressed as the Fourier series

$$C(t,x)=\frac{1}{2}+\sum_{n=0}^{\infty}\frac{\mathrm{e}^{-\lambda_n^4 t}\sin\lambda_n x}{\lambda_n} \tag{29}$$

where

$$\lambda_n=\frac{\pi}{2}+n\pi \tag{30}$$

Funnily enough, Merryfield and Holloway (2003) explain that the overshootings '*are not a Gibbs' phenomenon, as they are insensitive to cut-off n provided they are sufficiently well resolved*'. This is true inasmuch as the overshootings are not associated with the truncation of the Fourier series or the attempt to represent a discontinuous distribution by means of a Fourier series. As we showed in the unbounded case, however, the overshootings are really similar to a Gibbs' phenomenon produced by the cut-off of the biharmonic mixing in the frequency domain.

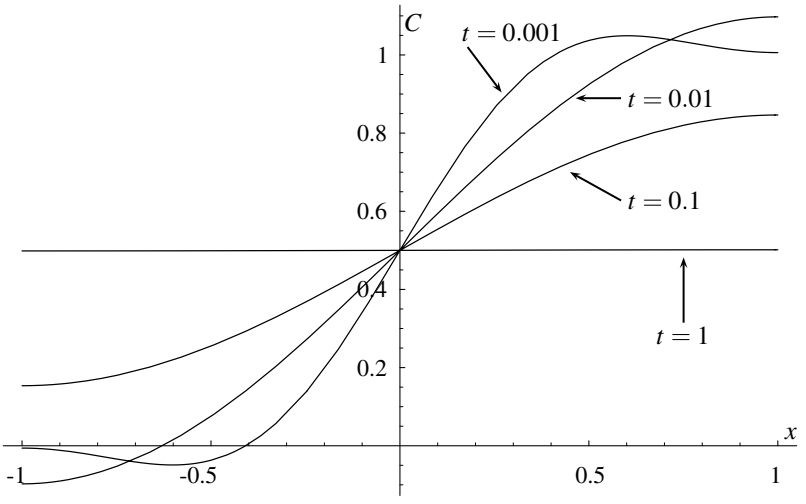


Fig. 6. Snapshots of the solution of the 1D biharmonic diffusion problem (28) in the bounded domain $x\in[-1,1]$.

## 6. Concluding remarks

During the last decade, biharmonic mixing has been increasingly used in large scale numerical models of the ocean (e.g. Willebrand et al., 2001; Xing and Davies, 2002; Lee and Coward, 2003; Myers and Deacu, 2004; Simmons et al., 2004; Oka and Hasumi, 2006; Shaw and Chao, 2006) because of its ability to damp numerical noise much more efficiently than Laplacian diffusion. As demonstrated and documented in this note, biharmonic mixing can however generate spurious oscillations and lacks positiveness.

Because of these unphysical aspects, the biharmonic formulation should not be regarded as a valid parameterization of diffusion. To avoid the confusion with the physical process of diffusion, the terminology "biharmonic mixing" should be preferred to the term "biharmonic diffusion" when referring to the effects of the biharmonic operator. Although seldom used, the expression "biharmonic filtering" provides however an even better description of the actual action of the biharmonic operator.

In practice, the solution will also be influenced by other processes which have not been taken into account above. Since the unwanted behaviours result from the very nature of the biharmonic term, one can argue that they will still show up in more complex situations, including those of spatially varying and anisotropic diffusion (e.g. Griffies and Hallberg, 2000).

The analysis carried out above suggests that the unphysical behaviour of biharmonic mixing may not be so critical in a range of practical situations. The understanding of overshootings and oscillations as a kind of Gibbs's phenomenon suggests indeed that the magnitude of the overshootings and oscillations will not grow unboundedly with time but will, on the contrary, remain below a few percents of the original perturbation. Such a behaviour can also be anticipated from the monotonic decrease of the total variance of the field (if appropriate boundary conditions are applied).

In a way, biharmonic diffusion behaves similarly to total variation diminishing (TVD) advection schemes (Harten, 1983). In both cases, the development of oscillations and overshootings are constrained by the condition that, respectively, the total variance or the total variation decreases. For TVD schemes, the constraint is strong enough to enforce monotonicity (Harten, 1983). This is not the case, however, for biharmonic mixing.

The assessment of the importance of the overshootings and spurious oscillations is different if the biharmonic operator is used to parameterize the mixing of momentum or if is applied to scalar tracers.

Overshootings and oscillations induced by biharmonic friction can be seen as a price to pay to get most of the dissipation of kinetic energy at the smaller scale and to keep the advective aspects of the main flow. In this context of the mixing of momentum, the peculiar behaviour of the biharmonic operator can be found acceptable in many studies. This is however by no means the only feasible approach to avoid spurious diffusion. High-order advection schemes and other models like horizontally anisotropic diffusion of momentum can be used to enhance the flow energetics in a more physical way (e.g. Smith and McWilliams, 2003; Smith and Gent, 2004; Griffies, 2004).

Because of its clear influence on the generation and development of local maxima and oscillations, the use of biharmonic mixing should be avoided in analytical and numerical studies dealing with the genesis of instabilities (e.g. Wu and Haines, 1998; Simmons et al., 2004); biharmonic mixing can influence the initiation and development of the instabilities in an unphysical way.

The use of biharmonic mixing for tracers (e.g. Oschlies, 2001; Willebrand et al., 2001; Crispi et al., 2002; Machu et al., 2005; Losa et al., 2006) is more problematic. The lack of positiveness appears indeed as a severe drawback since negative values of the concentration are, of course, inacceptable. The biharmonic mixing should therefore be used with care in the context of tracer studies. In biological models, the overshootings are particularly critical because they can be amplified by the dynamics of the system – a problem that is already recognized for imperfectly rotated Laplacian diffusion operator (Beckers et al., 1998; Gnanadesikan, 1999; Beckers et al., 2000).

## Acknowledgments

E. Delhez and E. Deleersnijder are respectively honorary Research Associate and Research Associate with the Belgian National Fund for Scientific Research (F.N.R.S.).

This paper is MARE Publication No. 106.

Part of this study was carried out in the scope of the development of the second-generation Louvain-la-Neuve Ice-Ocean Model (SLIM, www.climate.be/SLIM), which is funded by the Communauté Française de Belgique under Contract ARC 04/09-316.

## Appendix A. Analytical solution of the differential problem (7)

The solution of the differential problem (7) can be obtained in two steps.

First we compute the Green function $\mathscr{G}$ associated with this differential problem, i.e. the solution of

$$\begin{cases} \dfrac{\partial \mathscr{G}}{\partial t} = -\kappa_4 \dfrac{\partial^4 \mathscr{G}}{\partial x^4} \\ \mathscr{G}(0,x) = \delta(x) \end{cases} \tag{A.1}$$

where $\delta$ is the Dirac impulse generalized function. The problem can be solved using the Fourier transform approach described in the main text. The Fourier transform of the initial condition is

$$\widetilde{\mathscr{G}}(0,k) = \frac{1}{\sqrt{2\pi}} \tag{A.2}$$

and the solution is readily obtained as

$$\widetilde{\mathscr{G}}(t,k) = \frac{1}{\sqrt{2\pi}} \mathrm{e}^{-\kappa_4 k^4 t} \tag{A.3}$$

The Green function is computed by inverting the Fourier transform. Using Mathematica®, one gets

$$\mathscr{G}(t,x) = \frac{1}{8\pi(\kappa_4 t)^{3/4}} \left\{ 2\sqrt{\kappa_4 t}\,\Gamma\left(\frac{1}{4}\right) {}_0F_2\left(;\frac{1}{2},\frac{3}{4};\frac{x^4}{256\kappa_4 t}\right) - x^2\Gamma\left(\frac{3}{4}\right) {}_0F_2\left(;\frac{5}{4},\frac{3}{2};\frac{x^4}{256\kappa_4 t}\right) \right\} \tag{A.4}$$

where ${}_0F_2$ is a generalized hypergeometric function.

In a second step, the solution of (7) for arbitrary initial conditions can be computed as

$$C(t,x) = \int_{-\infty}^{\infty} C_0(\xi)\mathscr{G}(t,x-\xi)\,\mathrm{d}\xi \tag{A.5}$$

## Appendix B. Green function of the multi-dimensional isotropic diffusion problem

Using the scaling introduced in (18), the $n$-dimensional (where $n = 1$, 2 or 3) version of the isotropic diffusion problem with both Laplacian and biharmonic diffusion terms can be stated as

$$\begin{cases} \dfrac{\partial \mathscr{G}_n}{\partial t_\star} = \nabla_\star^2 \mathscr{G}_n - \nabla_\star^4 \mathscr{G}_n \\ \mathscr{G}_n(0,\mathbf{x}_\star) = \sqrt{\dfrac{\kappa_2}{\kappa_4}}\delta(\mathbf{x}_\star) \end{cases} \tag{B.1}$$

where $\nabla_\star^2$ and $\nabla_\star^4$ are the appropriate $n$-dimensional differential operator in dimensionless variables.

The $n$-dimensional Fourier transform of the problem leads to

$$\begin{cases} \dfrac{\partial \widetilde{\mathscr{G}}_n}{\partial t_\star} + (k_\star^2 + k_\star^4)\widetilde{\mathscr{G}}_n = 0 \\ \widetilde{\mathscr{G}}_n(0,\mathbf{k}_\star) = \frac{1}{(2\pi)^{n/2}}\sqrt{\dfrac{\kappa_2}{\kappa_4}} \end{cases} \tag{B.2}$$

where $\mathbf{k}_\star$ is the $n$-dimensional wave vector and $k_\star = |\mathbf{k}_\star|$.

The Fourier transform of the Green function is therefore given by

$$\widetilde{\mathscr{G}}_n(t_\star,\mathbf{k}_\star) = \frac{1}{(2\pi)^{n/2}}\sqrt{\frac{\kappa_2}{\kappa_4}}\mathrm{e}^{-(k_\star^2+k_\star^4)t_\star} \tag{B.3}$$

and

$$\mathscr{G}_n(t_\star, \mathbf{x}_\star) = \mathscr{F}^{-1}_{\mathbf{x}_\star}[\widetilde{\mathscr{G}}_n(t_\star, \mathbf{k}_\star)] = \frac{1}{(2\pi)^n}\sqrt{\frac{\kappa_2}{\kappa_4}}\int_{\mathbb{R}^n} \mathrm{e}^{\mathrm{i}\mathbf{k}_\star\cdot\mathbf{x}_\star - (k_\star^2+k_\star^4)t_\star}\,\mathrm{d}\mathbf{k}_\star \tag{B.4}$$

In the one-dimensional case, one gets

$$\mathscr{G}_1(t_\star, x_\star) = \frac{1}{\pi}\sqrt{\frac{\kappa_2}{\kappa_4}}\int_0^{+\infty} \cos(k_\star x_\star)\mathrm{e}^{-(k_\star^2+k_\star^4)t_\star}\,\mathrm{d}k_\star \tag{B.5}$$

In two dimensions, taking into account the radial symmetry of $\mathscr{G}_2$ and using the integral representation of the Bessel function of the first kind

$$J_0(\alpha) = \frac{1}{2\pi}\int_0^{2\pi} \mathrm{e}^{\mathrm{i}\alpha\cos\theta}\,\mathrm{d}\theta, \quad (\alpha > 0) \tag{B.6}$$

one gets

$$\mathscr{G}_2(t_\star, r_\star) = \frac{1}{2\pi}\sqrt{\frac{\kappa_2}{\kappa_4}}\int_0^{+\infty} k_\star J_0(r_\star k_\star)\mathrm{e}^{-(k_\star^2+k_\star^4)t_\star}\,\mathrm{d}k_\star \tag{B.7}$$

where $r_\star = |\mathbf{x}_\star|$.

In the three-dimensional case, using the spherical symmetry, the Green function can be expressed as

$$\mathscr{G}_3(t_\star, r_\star) = \frac{1}{2\pi^2 r_\star}\sqrt{\frac{\kappa_2}{\kappa_4}}\int_0^{+\infty} k_\star \sin(r_\star k_\star)\mathrm{e}^{-(k_\star^2+k_\star^4)t_\star}\,\mathrm{d}k_\star \tag{B.8}$$

## Appendix C. Discrete Green function of the 1D mixed diffusion problem

In the 1D discrete case, one considers the problem

$$\begin{cases} \dfrac{\partial \mathscr{G}_j}{\partial t} = \dfrac{\kappa_2}{\Delta^2}[\mathscr{G}_{j+1} - 2\mathscr{G}_j + \mathscr{G}_{j-1}] - \dfrac{\kappa_4}{\Delta^4}[\mathscr{G}_{j+2} - 4\mathscr{G}_{j+1} + 6\mathscr{G}_j - 4\mathscr{G}_{j-1} + \mathscr{G}_{j-2}] \\ \mathscr{G}_j(0) = \frac{1}{\Delta}\delta(j) \end{cases} \tag{C.1}$$

To solve this problem, one can take the discrete time Fourier transform with respect to $j$, i.e.

$$\widetilde{\mathscr{G}}(t,k) = \sum_{j=-\infty}^{+\infty} \mathscr{G}_j(t)\mathrm{e}^{-\mathrm{i}kj} \tag{C.2}$$

The difference problem transforms to

$$\begin{cases} \dfrac{\partial \widetilde{\mathscr{G}}}{\partial t} = -\left[\dfrac{4\kappa_2\sin^2(k/2)}{\Delta^2} + \dfrac{16\kappa_4\sin^4(k/2)}{\Delta^4}\right]\widetilde{\mathscr{G}} \\ \widetilde{\mathscr{G}}(0,k) = \frac{1}{\Delta} \end{cases} \tag{C.3}$$

The solution is therefore given by

$$\widetilde{\mathscr{G}}(t,k) = \frac{1}{\Delta}\exp\left(-\left[\frac{4\kappa_2\sin^2(k/2)}{\Delta^2} + \frac{16\kappa_4\sin^4(k/2)}{\Delta^4}\right]t\right) \tag{C.4}$$

hence

$$\begin{aligned} \mathscr{G}_j(t) &= \frac{1}{2\pi\Delta}\int_{-\pi}^{+\pi} \exp\left(-\left[\frac{4\kappa_2\sin^2(k/2)}{\Delta^2} + \frac{16\kappa_4\sin^4(k/2)}{\Delta^4}\right]t\right)\mathrm{e}^{\mathrm{i}kj}\,\mathrm{d}k \\ &= \frac{1}{\pi\Delta}\int_0^{+\pi} \exp\left(-\left[\frac{4\kappa_2\sin^2(k/2)}{\Delta^2} + \frac{16\kappa_4\sin^4(k/2)}{\Delta^4}\right]t\right)\cos(kj)\,\mathrm{d}k \end{aligned} \tag{C.5}$$

## Appendix D. Variance of the field

Consider the initial value problem (22) with the assumption that the closed surface $\Gamma$ is impermeable, i.e.

$$\mathbf{u}\cdot\mathbf{n}=0 \quad \text{on } \Gamma \tag{D.1}$$

and the divergence of the velocity field is zero, i.e.

$$\nabla\cdot\mathbf{u}=0 \tag{D.2}$$

The boundary condition (23) ensures that the integrated flow of material across $\Gamma$ is zero. Hence, the basin average concentration $\overline{C}$ is a constant (which can be computed by averaging the initial concentration field).

The deviation $\widehat{C}=C-\overline{C}$ of the concentration with respect to its basin average value satisfy the differential equation

$$\frac{\partial\widehat{C}}{\partial t}=-\nabla\cdot\{\mathbf{u}\widehat{C}-\mathbf{K}\cdot\nabla\widehat{C}+\nabla(\kappa_4\nabla^2\widehat{C})\} \tag{D.3}$$

From this differential equation, straightforward, but tedious, analytical manipulations lead to

$$\frac{1}{2}\frac{\partial\widehat{C}^2}{\partial t}=-\frac{1}{2}\nabla\cdot(\mathbf{u}\widehat{C}^2)+\nabla\cdot\left\{\widehat{C}[\mathbf{K}\cdot\nabla\widehat{C}-\nabla(\kappa_4\nabla^2\widehat{C})]\right\}-\nabla\widehat{C}\cdot\mathbf{K}\cdot\nabla\widehat{C}+\nabla\cdot[\nabla\widehat{C}(\kappa_4\nabla^2\widehat{C})]-\kappa_4(\nabla^2\widehat{C})^2 \tag{D.4}$$

Using the divergence theorem, the integration of this equation over the domain $V$ yields (25) if the conditions (D.1) and (23) are taken into account to cancel the surface integrals associated with the two first terms of the right-hand-side of the equation.

Note that this result is obtained without any assumption on $\kappa_4$. In particular, the result is valid if $\kappa_4$ varies in space and time.

## Appendix E. Positiveness of the diffusion operator

Consider again the advection–diffusion problem (22) in the domain $V$ with the boundary conditions (23) and (D.1) prescribed on the boundary surface $\Gamma$.

Let $C_-$ be the negative part of the concentration field $C$, i.e.

$$C_-=\frac{|C|-C}{2} \tag{E.1}$$

Obviously, $C_-$ is zero if $C$ is positive and is equal to $-C$ if $C$ is negative. Let $V_-$ denote the sub-domain of $V$ where $C<0$ or, equivalently, $C_->0$. In the following, we will try to prove that the concentration is everywhere positive by showing that the measure of $V_-$ is zero (Deleersnijder et al., 2001).

Let $\mathbf{n}_-$ be the outward unit normal of the boundary $\Gamma_-$ of $V_-$. Note that $\Gamma_-$ can be split into two disjoint parts corresponding respectively to the intersection $\Gamma_-\cap\Gamma$ of $\Gamma_-$ with $\Gamma$ and the part $\Gamma_-\backslash\Gamma$ of $\Gamma_-$ which runs through the interior of $V$ and on which $C=C_-=0$.

Multiplying (22) by $C_-$ and integrating over $V$ yields

$$\int_V C_-\frac{\partial C}{\partial t}\,\mathrm{d}V=-\int_V C_-\nabla\cdot(\mathbf{u}C)\,\mathrm{d}V+\int_V C_-\nabla\cdot(\mathbf{K}\cdot\nabla C)\,\mathrm{d}V-\int_V C_-\nabla\cdot[\nabla(\kappa_4\nabla^2C)]\,\mathrm{d}V \tag{E.2}$$

Taking into account the fact that $C_-$ is zero outside $V_-$, using the Reynolds' transport theorem to account for possible movements of $\Gamma_-$, the left-hand side successively transforms to

$$\int_V C_-\frac{\partial C}{\partial t}\,\mathrm{d}V=-\int_{V_-}C_-\frac{\partial C_-}{\partial t}\,\mathrm{d}V_-=-\frac{1}{2}\int_{V_-}\frac{\partial C_-^2}{\partial t}\,\mathrm{d}V_-=-\frac{1}{2}\frac{\mathrm{d}}{\mathrm{d}t}\int_{V_-}C_-^2\,\mathrm{d}V_--\int_{\Gamma_-}(\mathbf{v}_-\cdot\mathbf{n}_-)C_-^2\,\mathrm{d}\Gamma_1 \tag{E.3}$$

where $\mathbf{v}_-$ is the velocity at which $\Gamma_-$ moves. The last integral in (E.3) vanishes because $\mathbf{v}_-$ is zero on $\Gamma_- \cup \Gamma$ (the surface is fixed) and because $C_-$ is zero on that part of $\Gamma_1$ that runs trough the interior of $V$. One has therefore

$$\int_V C_- \frac{\partial C}{\partial t}\,\mathrm{d}V = -\frac{1}{2}\frac{\mathrm{d}}{\mathrm{d}t}\int_{V_-} C_-^2\,\mathrm{d}V_- \tag{E.4}$$

The first integral in the right-hand side of (E.2) can be transformed as follows:

$$-\int_V C_-\nabla\cdot(\mathbf{u}C)\,\mathrm{d}V = \frac{1}{2}\int_{V_-}\nabla\cdot(\mathbf{u}C_-^2)\,\mathrm{d}V_- = \frac{1}{2}\int_{\Gamma_-}(\mathbf{u}\cdot\mathbf{n}_-)C_-^2\,\mathrm{d}\Gamma_- = 0 \tag{E.5}$$

because either $(\mathbf{u}\cdot\mathbf{n}_-)$ or $C_-$ is zero on the two parts of $\Gamma_1$.

The second integral in the right-hand side of (E.2) can be written as

$$\begin{aligned}\int_V C_-\nabla\cdot(\mathbf{K}\cdot\nabla C)\,\mathrm{d}V &= \int_{V_-}\nabla C\cdot\mathbf{K}\cdot\nabla C\,\mathrm{d}V_- - \int_{V_-}\nabla\cdot(C\mathbf{K}\cdot\nabla C)\,\mathrm{d}V_- \\ &= \int_{V_-}\nabla C\cdot\mathbf{K}\cdot\nabla C\,\mathrm{d}V_- - \int_{\Gamma_-}\mathbf{n}_-\cdot(C\mathbf{K}\cdot\nabla C)\,\mathrm{d}\Gamma_- = \int_{V_-}\nabla C\cdot\mathbf{K}\cdot\nabla C\,\mathrm{d}V_-\end{aligned} \tag{E.6}$$

if one takes into account that either $\mathbf{n}_-\cdot(\mathbf{K}\cdot\nabla C)$ or $C$ vanishes on $\Gamma_1$.

In the case of pure Laplacian diffusion ($\kappa_4 = 0$), injecting the intermediate results E.3–E.6 in (E.2) gives

$$\frac{\mathrm{d}}{\mathrm{d}t}\int_{V_-} C_-^2\,\mathrm{d}V_- = -2\int_{V_-}\nabla C\cdot\mathbf{K}\cdot\nabla C\,\mathrm{d}V_- \leqslant 0 \tag{E.7}$$

if $\mathbf{K}$ is positive definite. If the concentration field is everywhere positive at the initial time, one has $C_- = 0$ and the domain $V_-$ is empty, (E.7) shows that this will also be the case at any time. We conclude therefore that the concentration remains positive at any time and location.

When biharmonic mixing is present, the last term of the right-hand side of (E.2) must be considered as well. This transforms to

$$\begin{aligned}-\int_V C_-\nabla\cdot[\nabla(\kappa_4\nabla^2 C)]\,\mathrm{d}V &= \int_{V_-} C\nabla\cdot[\nabla(\kappa_4\nabla^2 C)]\,\mathrm{d}V_- \\ &= \int_{V_-}\{\nabla\cdot[C\nabla(\kappa_4\nabla^2 C)] - \nabla\cdot[\nabla C(\kappa_4\nabla^2 C)] + \kappa_4(\nabla^2 C)^2\}\,\mathrm{d}V_- \\ &= \int_{\Gamma_-} C\mathbf{n}_-\cdot\nabla(\kappa_4\nabla^2 C)\,\mathrm{d}\Gamma_1 - \int_{\Gamma_-}(\mathbf{n}_-\cdot\nabla C)(\kappa_4\nabla^2 C)\,\mathrm{d}\Gamma_1 \\ &\quad + \int_{V_-}\kappa_4(\nabla^2 C)^2\,\mathrm{d}V_-\end{aligned} \tag{E.8}$$

The first integral on the right-hand side vanishes because either $C$ or $\mathbf{n}_-\cdot\nabla(\kappa_4\nabla^2 C)$ is zero on $\Gamma_-$. The contribution of $\Gamma_-\cap\Gamma$ to the second integral is also zero because of (27). Eq. (E.2) becomes therefore

$$\frac{\mathrm{d}}{\mathrm{d}t}\int_{V_-} C_-^2\,\mathrm{d}V_- = -2\int_{V_-}\nabla C\cdot\mathbf{K}\cdot\nabla C\,\mathrm{d}V_- + 2\int_{\Gamma_-\setminus\Gamma}\mathbf{n}_-\cdot(\kappa_4\nabla C)\nabla^2 C\,\mathrm{d}\Gamma_1 - 2\int_{V_-}\kappa_4(\nabla^2 C)^2\,\mathrm{d}V_- \tag{E.9}$$

This expression would allow to conclude that the negative part of the concentration field decreases with time if the surface integral on the right-hand side would vanish. Unfortunately, there is no reason for this to occur and negative values of the concentration cannot be ruled out. Such negatives values are indeed apparent in Fig. 6. Since the surface integral only depends on $\kappa_4$, not $\mathbf{K}$, (E.9) also suggests that, as shown in Fig. 3, Laplacian diffusion cannot help to avoid the undershootings induced by the biharmonic term.

## References


Batteen, M.L., Martinez, J.R., Bryan, D.W., Buch, E.J., 2000. A modelling study of the coastal eastern boundary current system off Iberia and Morocco. Journal of Geophysical Research 105, 14173–14195.

Beckers, J.-M., Burchard, H., Campin, J.-M., Deleersnijder, E., Mathieu, P.P., 1998. Another reason why simple discretizations of rotated diffusion operators cause problems in ocean models: comments on 'Isoneutral diffusion in a $z$-coordinate ocean model'. Journal of Physical Oceanography 28 (7), 1552–1559.

Beckers, J.-M., Burchard, H., Deleersnijder, E., Mathieu, P.P., 2000. Numerical discretization of rotated diffusion operators in ocean models. Monthly Weather Review 128 (8), 2711–2733.

Crispi, G., Crise, A., Solidoro, C., 2002. Coupled Mediterranean ecomodel of the phosphorus and nitrogen cycles. Journal of Marine Systems 33–34, 497–521.

Deleersnijder, E., Campin, J.-M., Delhez, E.J.M., 2001. The concept of age in marine modelling I. Theory and preliminary model results. Journal of Marine Systems 28 (3–4), 229–267.

DiBattista, M.T., Majda, A.J., Grote, M.J., 2001. Meta-stability of equilibrium statistical structures for prototype geophysical flows with damping and driving. Physica D 151, 271–304.

Foujols, M.-A., Lévy, C., Aumont, O., Madec, G., 2000. OPA 8.1 Tracer Model reference Manual. Note technique du pôle de modélisation, Institut Pierre Simon Laplace, IPSL. http://www.lodyc.jussieu.fr/opa/.

Gent, P.R., McWilliams, J.C., 1990. Isopycnal mixing in ocean circulation models. Journal of Physical Oceanography 20, 150–155.

Gent, P.R., Willebrand, J., McDougall, T.J., McWilliams, J.C., 1995. Parameterizing eddy-induced tracer transports in ocean circulation models. Journal of Physical Oceanography 25, 463–474.

Gnanadesikan, A., 1999. Numerical issues for coupling biological models with isopycnal mixing schemes. Ocean Modelling 1 (1), 1–15.

Griffies, S.M., Hallberg, R.W., 2000. Biharmonic friction with a Smagorinsky-like viscosity for use in large-scale eddy-permitting ocean models. Monthly Weather Review 128, 2935–2946.

Griffies, S.M., 2004. Fundamentals of Ocean Climate Models. Princeton University Press, Princeton and Oxford, 518 pp.

Griffies, S.M., Harrison, M.J., Pacanowski, R.C., Rosati, A., 2004. A technical guide to MOM4. GFDL Ocean Group Technical Report No. 5, NOAA/Geophysical Fluid Dynamics Laboratory. Available from: www.gfdl.noaa.gov.

Harten, A., 1983. High resolution schemes for hyperbolic conservation laws. Journal of Computational Physics 49, 357–393.

Holland, W.R., Chow, J.C., Bryan, F.O., 1998. Application of a third-order upwind scheme in the NCAR ocean model. Journal of Climate 11, 1487–1493.

Hunke, E.C., Lysne, J.A., Hecht, M.W., Maltrud, M.E., 2005. GM vs biharmonic ocean mixing in the Arctic. Institute of Physics Publishing, Journal of Physics: Conference Series 16, 348–352. doi:10.1088/1742-6596/16/1/048.

Lee, M.-M., Coward, A., 2003. Eddy mass transport for the Southern Ocean in an eddy-permitting global ocean model. Ocean Modelling 5 (3), 249–266.

Leonard, B.P., 1979. A stable and accurate convective modelling procedure based on quadratic upstream interpolation. Computational Methods in Applied Mechanics and Engineering 19, 59–98.

Losa, S.N., Vézina, A., Wright, D., Lu, Y., Thompson, K., Dowd, M., 2006. 3D ecosystem modelling in the North Atlantic: relative impacts of physical and biological parameterizations. Journal of Marine Systems 61 (3–4), 230–245.

Machu, E., Biastoch, A., Oschlies, A., Kawamiya, M., Lutjeharms, J.R.E., Garçon, V., 2005. Phytoplankton distribution in the Agulhas system from a coupled physical–biological model. Deep Sea Research Part I: Oceanographic Research Papers 52 (7), 1300–1318.

Madec, G., Chartier, M., Delecluse, P., Crépon, M., 1991. A three dimensional numerical study of deep water formation in the northwestern Mediterranean Sea. Journal of Physical Oceanography 21, 1349–1371.

Madec, G., Delecluse, P., Imbard, M., Lévy, C., 1999. OPA8.1 Ocean General Circulation Model Reference Manual, Note du Pôle de modélisation, Institut Pierre Simon Laplace. http://www.lodyc.jussieu.fr/opa/.

Merryfield, W.J., Holloway, G., 2003. Application of an accurate advection algorithm to sea-ice modelling. Ocean Modelling 5 (1), 1–15.

Morse, P.M., Feshbach, H., 1953. Methods of Theoretical Physics – Part I. Mc Graw-Hill, 997 pp.

Myers, P.G., Deacu, D., 2004. Labrador sea freshwater content in a model with a partial cell topographic representation. Ocean Modelling 6 (3–4), 359–377.

Oka, A., Hasumi, H., 2006. Effects of model resolution on salt transport through northern high-latitude passages and Atlantic meridional overturning circulation. Ocean Modelling 13 (2), 126–147.

Oschlies, A., 2001. Model-derived estimates of new production: new results point towards lower values. Deep Sea Research Part II: Topical Studies in Oceanography 48 (10), 2173–2197.

Semtner, A.J., Mintz, A., 1977. Numerical simulation of the Gulf Stream and mid-ocean eddies. Journal of Physical Oceanography 7, 208–230.

Shaw, P.-T., Chao, S.-Y., 2006. A nonhydrostatic primitive-equation model for studying small-scale processes: an object-oriented approach. Continental Shelf Research 26 (12–13), 1416–1432.

Simmons, H.L., Hallberg, R.W., Arbic, B.K., 2004. Internal wave generation in a global baroclinic tide model. Deep Sea Research Part II: Topical Studies in Oceanography 51 (25–26), 3043–3068.

Smith, R., Gent, P., 2002. Reference manual for the Parallel Ocean Program (POP). Technical Report LAUR-02-2484. Los Alamos National Laboratory, Los Alamos, New Mexico.

Smith, R.D., Gent, P.R., 2004. Anisotropic GM parameterization for ocean models. Journal of Physical Oceanography 34 (11), 2541–2564.

Smith, R.D., McWilliams, J.C., 2003. Anisotropic horizontal viscosity for ocean models. Ocean Modelling 5, 129–156.

Titz, S., Kuhlbrodt, T., FeudelGrid, U., 2004. Geometry effects on convection in ocean climate models: a conceptual study. Ocean Modelling 7 (1–2), 165–181.

Webb, D.J., de Cuevas, B.A., Richmond, C.S., 1998. Improved advection schemes for ocean models. Journal of Atmospheric and Oceanic Technology 15, 1171–1187.

Willebrand, J., Barnier, B., Böning, C., Dieterich, Ch., Killworth, P.D., Le Provost, Ch., Jia, Y., Molines, J.M., New, A.L., 2001. Circulation characteristics in three eddy-permitting models of the North Atlantic. Progress in Oceanography 48 (2–3), 123–161.

Wu, P., Haines, K., 1998. The general circulation of the Mediterranean Sea from a 100-years simulation. Journal of Geophysical Research 103 (C1), 1121–1135.

Xing, J., Davies, A.M., 2002. Influence of shelf topography upon along shelf flow and across shelf exchange in the region of the Ebro Delta. Continental Shelf Research 22 (10), 1447–1475.